Available online at www.sciencedirect.com
ScienceDirect
Catalysis Today 119 (2007) 120–124
CATALYSIS TODAY
www.elsevier.com/locate/cattod

Spectroscopic EPR and IR studies of monomeric and dimeric species formed upon adsorption of nitric oxide on $Ce_{0.75}Zr_{0.25}O_2$ and their reactivity with dioxygen

Andrzej Adamski [a,*], Gérald Djéga-Mariadassou [b], Zbigniew Sojka [a,c]

[a] *Jagiellonian University, Faculty of Chemistry, Ingardena 3, 30-060 Cracow, Poland*
[b] *UPMC, LRS, 4 Pl. Jussieu, 75252 Paris Cedex 05, France*
[c] *Regional Laboratory of Physicochemical Analyses and Structural Research, Ingardena 3, 30-060 Cracow, Poland*

Available online 15 September 2006

Abstract

The interaction of nitric oxide with $Ce_{0.75}Zr_{0.25}O_2$ solid solution were investigated by means of EPR and IR spectroscopies. The influence of adsorption parameters such as adsorption temperature and pressure, presence of the O_2 co-reactant on the nature and relative surface abundance of the resultant mono- and dimeric NO species was elucidated. The thermal stability of the surface nitrosyl complexes and their reactivity toward dioxygen were also examined.

Keywords: $Ce_{0.75}Zr_{0.25}O_2$; NO; Mononitrosyls; Dimers, EPR; IR

1. Introduction

The removal of noxious NO_x produced by combustion in mobile and stationary sources is one of the most significant environmental issues. In spite of the great experimental and theoretical effort, a satisfactory solution of this problem has still not been found [1–5]. Incomplete understanding of the deNO_x process in the presence of ubiquitous contaminant molecules such as oxygen and water, restrains the design of an efficient and industrially acceptable catalyst for reduction of NO_x to N_2 in lean-burn conditions. In this context, the interaction of nitrogen oxides with catalytic surfaces, owing to the variability in their coordination modes have received considerable interest, as it can provide hints for better understanding of the molecular pathways, along which NO can be decomposed or selectively reduced into elemental nitrogen [6–9]. For a relatively long time, selective catalytic reduction of NO_x by NH_3 was considered to be the most attractive route for NO_x abatement. At present, however, the attention is moved toward alternative reductants like small hydrocarbon molecules, such as CH_4, C_2H_4, C_3H_6 or C_3H_8 [2,3,10] or alcohols (CH_3OH, C_2H_5OH) [11].

In the gas phase NO molecule is EPR-silent in its $^2\Pi_{1/2}$ ground state due to the degeneracy of both π^* orbitals. Such degeneracy is removed upon adsorption, when NO interacts with the adsorption site. Since the g_z component is the most sensitive to the surface crystal field generated at the metal ion center, the NO molecule can be used as a probe for investigation of the active sites on the surface of heterogeneous catalysts.

Cerium dioxide, a common additive in the TWCs, can act as an oxygen storage component, participating directly in nitric oxide reduction [12,13]. In this context it is also worth examining the mechanism of NO interaction with binary ZrO_2–CeO_2 systems. As emphasized by many authors, one of the crucial steps of deNO_x reaction is the way of NO adsorption [3,14,15].

The aim of this work is focused on identification of surface NO-containing species formed during low- and high-temperature interaction of NO with the surface of $Ce_{0.75}Zr_{0.25}O_2$ solid solutions and determination of their transformation pathways in the presence of dioxygen at low pressures.

* Corresponding author.
E-mail address: adamski@chemia.uj.edu.pl (A. Adamski).

0920-5861/$ – see front matter © 2006 Elsevier B.V. All rights reserved.
doi:10.1016/j.cattod.2006.08.004

2. Experimental

The investigated CeO_2–ZrO_2 solid solutions, containing 75 mol% of CeO_2, were provided by RHODIA and obtained *via* simple hydrothermal synthesis from nitrate precursors, dried at 373 K for 1 h and then calcined at 873 K for 6 h.

The investigated samples were structurally and texturally characterized by XRD, SEM/TEM, and N_2-porosimetry. Their spectroscopic characterization by EPR, IR and Raman was also performed. In the present paper mainly IR and EPR results will be discussed.

The IR spectra were collected with an Equinox 55 spectrometer, equipped with an MCT detector, at spectral resolution of 2 cm^{-1}. Samples placed on the silicon wafers were treated *in situ* in an IR cell. CW-EPR X-band spectra were recorded at room and liquid nitrogen (77 K) temperatures with a Bruker ELEXSYS E-500 spectrometer operating at 100 kHz field modulation. EPR parameters were determined by using an EPRsim32 simulation program [16].

Nitric oxide was adsorbed at the pressures of 2–20 Torr on the samples previously outgassed under vacuum ($p \leq 10^{-5}$ Torr) and activated at 623–673 K for 0.5 h. The investigated samples were contacted with NO at 77 K for 1 min and next gradually exposed to room temperature to follow the adsorption progress. The latter process was monitored by EPR. In some cases higher activation temperatures up to 673 K were applied. Once the NO evolution was accomplished, the samples were outgassed and in some cases oxygen was introduced at 77 K, then the exposure to room temperature was repeated.

3. Results and discussion

After low-temperature (77 K) adsorption of NO onto $Ce_{0.75}Zr_{0.25}O_2$ solid solutions the reaction progress was monitored by the EPR as a function of p_{NO} and time of exposure to room temperature. At NO pressures of 2–5 Torr, one can observe a broad ($\Delta B_{pp} \approx 20$ mT) asymmetric signal at $g_{av} \approx 1.99$, which dominated the EPR spectrum (Fig. 1a). Only the traces of the ^{14}N ($I = 1$) hyperfine structure (hfs) could be detected in some cases. This signal was attributed to NO molecules loosely bound to the surface of $Ce_{0.75}Zr_{0.25}O_2$, similarly to those observed previously after NO adsorption on ceria-lean samples (e.g. $Ce_{0.20}Zr_{0.80}O_2$) [17]. A noteworthy feature of this signal is a distinct negative shift (with respect to the g_e value) of the g_z component, indicating that the unpaired electron is largely localized on the NO moiety. Indeed, at first approximation such g value can be rationalized in terms of a perturbed $^2\Pi_{1/2}$ radical with the unpaired electron confined to one of the two π_g^* orbitals, the degeneracy of which has been removed as a result of the NO coordination to the surface centers. The orbital momentum about the ligand internuclear axis is then partially quenched, making the EPR observation of bound NO possible. The local symmetry of the resultant surface complex must be orthorhombic (or lower), since an axial crystal field cannot lift the degeneracy of the π_g^* levels. This rules out a linear geometry of the coordination, indicating that the bound NO exhibits a bent η^1 or side-on η^2 structure. The ^{14}N hfs was not resolved in this case, partly because the spectra were too broad in the perpendicular (x, y) region and due to their partially averaged character caused by a restricted motion of the surface trapped NO. As discussed elsewhere in more detail [18], such restricted mobility can decrease the nitrogen hyperfine structure, when the unpaired electron is on the orbital situated in the plane of the motion.

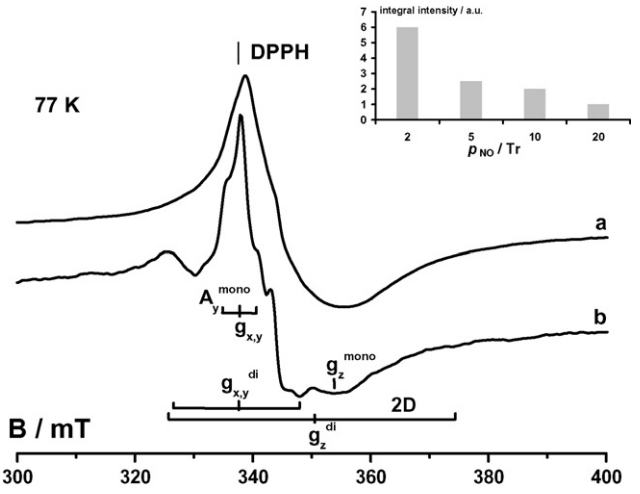

Fig. 1. EPR spectra of NO adsorbed at 77 K on the surface of $Ce_{0.75}Zr_{0.25}O_2$ solid solution under the pressure of: (a) $p_{NO} = 2$ Torr and (b) $p_{NO} = 20$ Torr. In the inset changes in the integral intensity of the EPR spectra as a function of p_{NO} are shown.

At higher NO pressures (20 Torr) enhanced resolution of the hfs lines along with appearance of new features attributable to $(NO)_2$ dimers were observed in the EPR spectrum (Fig. 1b), reflecting a complex pathway of NO interaction with the surface of $Ce_{0.75}Zr_{0.25}O_2$ samples. Such adsorption form seems to be preferred for all CeO_2–ZrO_2 samples containing more than 50 mol% of ceria [17]. The total amount of paramagnetic species decreased with increasing p_{NO}, as it can be inferred from the changes in the integral intensity of the EPR spectra (Fig. 1, inset).

A brief exposure of the $Ce_{0.75}Zr_{0.25}O_2$ sample with NO preadsorbed at 77 K to room temperature (150 s) led to distinct modification of the EPR signal and enhancement of the hyperfine structure resolution (Fig. 2). Computer simulation of this spectrum revealed that apart from a signal due to Zr^{3+} defects, two kinds of mononitrosyl complexes, stabilized on the zirconium and cerium ions could be distinguished. An orthorhombic signal with $g_x = 1.997$, $g_y = 2.000$, $g_z = 1.908$ and $|^N A_x|/g\beta_e = 3.1$ mT, can be attributed to a mononitrosyl ligand centered $\{Ce–NO\}^1$ surface complex, whereas the signal characterized by $g_x = 1.989$, $g_y = 1.999$, $g_z = 1.930$, $|^N A_x|/g\beta_e = 3.2$ mT, of distinctly higher g_z, to $\{Zr–NO\}^1$ surface complex (in Feltham and Enemark notation [19]). The components of the orthorhombic $\boldsymbol{g}$ tensor of the $\{Zr(Ce)–NO^\bullet\}^1$ species are given by the equations: $g_x = g_e + 2(\lambda/\Delta) - (\lambda/\delta)^2 + (\lambda/\delta)(\lambda/\Delta)$, $g_y = g_e - (\lambda/\delta)^2 - (\lambda/\delta)(\lambda/\Delta)$ and $g_z = g_e - 2(\lambda/\delta) + (\lambda/\delta)^3$, where λ is the spin–orbit coupling constant, and Δ and δ, the crystal field splitting parameters [20]. The shift in g_z value is directly related to splitting of both π^* levels by the adsorption site. Thus, if $g_z(Ce) < g_z(Zr)$, NO is

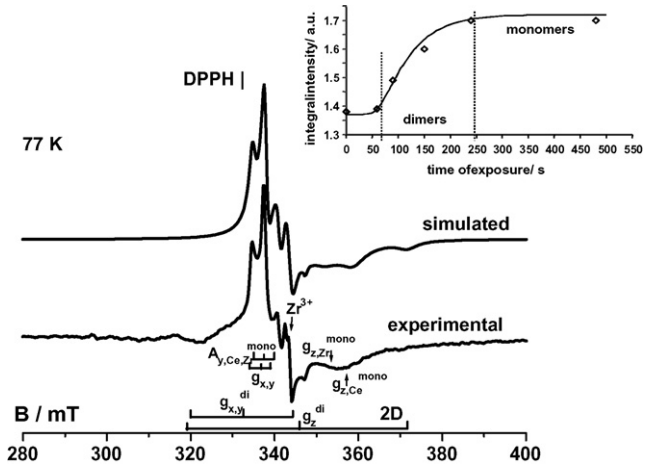

Fig. 2. Experimental and simulated EPR spectrum of $Ce_{0.75}Zr_{0.25}O_2$ after low-temperature (77 K) NO adsorption and subsequent exposition to room temperature for 150 s. In the inset changes in the intensity ratio between the signals from the mononitrosyls and dimers are shown as a function of the exposure time.

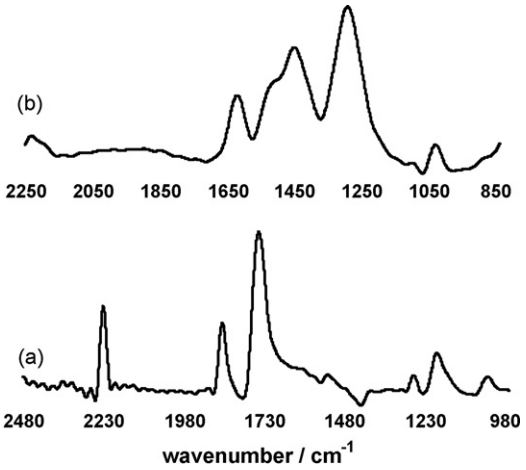

Fig. 3. Differential IR spectra of $Ce_{0.75}Zr_{0.25}O_2$ after (a) NO adsorption at 173 K (b) subsequent O_2 introduction at 293 K into the outgassed sample.

more strongly bound to cerium than to zirconium centers, confirming a more acidic Lewis character of Ce surface sites [21].

The signal with a distinct fine structure ($D \approx 22 \pm 1$ mT), originating from dipolar interaction between the unpaired electrons of two adjacent NO molecules can be ascribed to surface $(NO)_2$ dimers [20,22]. Since it was almost 2.5 times more intense than that of the mononitrosyl species, the bimolecular bonding of nitric oxide to the ceria-rich surface of $Ce_{0.75}Zr_{0.25}O_2$ seems to be a preferred way for NO adsorption at low temperatures.

The relative abundance of the EPR signals due to the surface mono- and dimeric species on the surface of $Ce_{0.75}Zr_{0.25}O_2$ is strongly influenced by adsorption temperature and pressure (Fig. 2, inset). On passing from 77 to 293 K, the population of dimeric species decreased from 71 to 54%, whereas the population of mononitrosyls increased from 18 to 43%, and the remaining part corresponds to the Zr^{3+} defects. Evidently, the dimeric complexes are less stable at elevated temperatures in comparison to the surface mononitrosyls, as it was previously reported for intrazeolite $Co^{2+}(NO)_2$ complexes in ZSM-5 [23]. Such behavior indicates that the binding energy of the second NO molecule ($\Delta E_{ads,2}$) has to be compensated by the gain in the translational and rotational entropy ($\Delta E_{ads,2} < T\,\Delta(S_{trans} + S_{rot})$), when the NO molecule is released upon the temperature jump.

The appearance of various nitrosyl surface complexes at low temperatures (173 K) was also confirmed by IR spectroscopy. The mononitrosyl complexes gave rise to an intense band at 1753 cm^{-1}, clearly observed in Fig. 3a. The position of this band, situated distinctly below the stretching mode of gaseous NO at 1876 cm^{-1} [24], is typical of nitroside $NO^{\delta-}$ species with a bent η^1-N structure [25]. Although at first glance it would suggest that the adsorption sites should consequently be partially oxidized upon NO adsorption, we think that the required electron density is rather supplied from the whole $Ce_{0.75}Zr_{0.25}O_2$ matrix *via* the metal adsorption center acting as a mere mediator [26]. Some adsorbed NO molecules formed strongly bent bridging surface complexes, as it can be inferred from the presence of a weaker band at 1200 cm^{-1} [24]. In addition, the appearance of a quite intense band at 1865 cm^{-1} is consistent with the presence of the loosely bound NO species, inferred from the EPR studies. At 173 K there are, however, no bands at around 1780 and 1870 cm^{-1}, previously observed on, e.g. sulfated zirconia [27] that could be attributed to $(NO)_2$ dinitrosyls. Instead we observed a pronounced band at 2235 cm^{-1} assigned to the ν(N–N) stretching in the N_2O molecule [24].

Upon exposure of the sample to room temperature for 60–90 s, the intensity of the EPR spectrum initially distinctly increased and then dramatically decreased with the elapsed time. This effect was especially strongly pronounced for lower NO pressures (2–5 Torr). Plausibly, at ambient temperatures part of the weakly bound NO molecules desorbed from the surface, whereas some of the dimeric $(NO)_2$ entities were transformed into N_2O, according to the equation: $2(NO)_2 = 2N_2O + O_2$, giving rise to an intense ν(N–N) band at ~2230 cm^{-1} and to a weak ν(N–O) band around ~1300 cm^{-1} [24]. Both of them were observed in the IR spectrum (not reported here) of NO adsorbed on $Ce_{0.75}Zr_{0.25}O_2$ recorded at temperature close to 273 K. Surface nitrous oxide can be produced *via* a hyponitrite $(O–N{=}N–O)^{2-}$ intermediate, proposed earlier by Martínez-Arias et al. in the case of ceria [12], which gives rise to a broad band at ~1315 cm^{-1} [24].

As it can be inferred from the EPR spectra presented in Fig. 4, in the absence of dioxygen, surface mononitrosyls were stable even up to 573 K. Indeed, after adsorption of excessive portion (*ca.* 10 Torr) of nitric oxide on $Ce_{0.75}Zr_{0.25}O_2$ at room temperature and subsequent heating of the sample to 413–513 K, the intensity of the corresponding EPR signal increased four times. This means that in such conditions, surface mononitrosyls can be easily formed and persist even at elevated temperatures.

Subsequent introduction of O_2 at 77 K under the pressure of 2 Torr to the CeO_2–ZrO_2 sample with preadsorbed NO caused dramatic changes in both the shape and the intensity of the

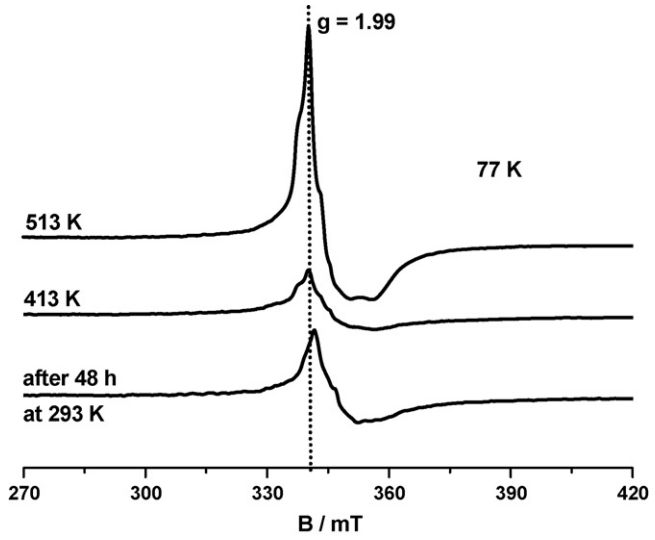

Fig. 4. Evolution of the EPR spectra of NO adsorbed on $Ce_{0.75}Zr_{0.25}O_2$ as a function of temperature (p_{NO} = 10 Torr).

EPR spectrum. The concentration of the surface mononitrosyl complexes strongly decreased, whereas the NO dimers were more reluctant to oxidation. The consumption of the mononitrosyls in the reaction with dioxygen was faster in comparison to dimers, reflecting their clearly different affinity toward gaseous O_2. Simultaneously, a new characteristic orthorhombic EPR signal appeared (Fig. 5), which was attributed to a superoxide ion with $^{1/2}\Pi_{3/2}$ ground state [28]. The $\boldsymbol{g}$ tensor values, found by computer simulation, $g_x = 2.012$, $g_y = 2.018$ and $g_z = 2.037$, confirmed the assignment of this signal to the O_2^- radical stabilized on tetravalent surface cations [29].

Obviously, the formation of a superoxide radical required an electron transfer from the surface to O_2 molecule, which usually is a thermally activated process. The necessary electrons may be supplied by the Ce^{3+} ions. In such case, the intensity of the O_2^- signal can be used to gauge $Ce_{0.75}Zr_{0.25}O_2$ surface defect structure. Production of surface defects upon thermal treatment is connected with relatively facile reduction of cerium, which is accompanied by creation

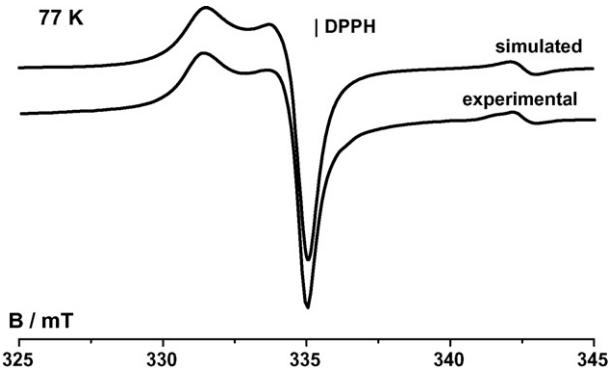

Fig. 5. Experimental and simulated spectrum of the O_2^-/Ce^{4+} surface complex recorded after low-temperature O_2 adsorption onto $NO/Ce_{0.75}Zr_{0.25}O_2$ (p_{O_2} = 2 Torr), and its subsequent exposition to room temperature for 1 min.

of oxygen vacancies ($V_O^{\bullet\bullet}$), according to the equation: $O_O^x + 2Ce_M^x \Leftrightarrow \frac{1}{2}O_{2(g)} + V_O^{\bullet\bullet} + 2Ce'_{(M)}$ (where Ce_M^x stands for Ce^{4+} and $Ce'_{(M)}$ for Ce^{3+} ions). Due to the fast spin–lattice relaxation, paramagnetic Ce^{3+} point defects, are extremely difficult to be detected by EPR at 77 K. However, in consequence of thermal activation of dioxygen onto CeO_2–ZrO_2 surface, the defects are scavenged in the following reaction: $Ce^{3+} + O_2 = Ce^{4+}$–O_2^- and finally O_2^- species can easily be detected by EPR even at room temperature.

Further exposure of the sample to room temperature for *ca.* 10 min, resulted in the remarkable decrease in intensity of the signal from O_2^-, together with the shift in its g_z value to 2.028. Such shift can be explained by the change of stabilization center of the O_2^-. The value of Δ parameter, describing the separation between the split 2p π_g energy levels and being a measure of surface stabilization, calculated from g_z shift, was equal 2.12 eV for O_2^-/Zr^{4+} and only 0.97 eV for O_2^-/Ce^{4+}. Apparently at elevated temperatures, O_2^- radicals can spill-over on CeO_2–ZrO_2 surface to be eventually stabilized on the Zr^{4+} cations. Additional evidence supporting formation of superoxide species exclusively in the presence of cerium was provided by the fact that O_2^- was not produced on *t*-ZrO_2, where after O_2 introduction only the physisorbed triplet state ($^3\Sigma_g^-$) dioxygen was detected.

Further stepwise exposition of the sample to room temperature and 373 K led to progressive decay of the EPR signal of O_2^- species. Most probably their reduction to diamagnetic O^{2-} took place together with simultaneous oxidation of surface NO species to surface nitrates according to the equation: $\{Ce^{4+}$–$O_2^-\}^1 + \{Ce^{4+}$–$NO\}^1 = Ce^{4+}$–NO_3^-–Ce^{4+}. Of course, instead of Ce^{4+} cations also Zr^{4+} cations can be engaged in this process.

Parallel IR investigations revealed that various nitrates were the final products of NO transformation on the surface of $Ce_{0.75}Zr_{0.25}O_2$ in the presence of dioxygen, giving rise to the strong bands in the region 1295–1625 cm^{-1} (Fig. 3b), typical of mono- and polydentate or bridging forms. Their particular attribution is not an easy task as most of the diagnostic bands overlap. Nevertheless, following literature, the band at 1625 cm^{-1} can be assigned to ν(N–O) stretching of the bridging nitrates, whereas the components at 1210 and the weak one at 1040 cm^{-1} to the $\nu_{as}(NO_2)$ and $\nu_s(NO_2)$ modes, respectively. The bidentate and monodentate NO_3^- contribute to the strong bands around 1530–1545 and 1275 cm^{-1}, whereas monodentate NO_2^- species gives rise to the band at 1460 cm^{-1} [24,27].

4. Conclusions

The interactions of NO and O_2 with $Ce_{0.75}Zr_{0.25}O_2$ solid solutions were investigated. The nature of the surface species formed upon NO adsorption was determined basing on the EPR and IR spectra. Their spectroscopic parameters were interpreted in terms of both mono- and dimeric NO surface complexes. Two different types of mononitrosyls, stabilized on zirconium and cerium cations, were found. At low temperatures dimeric species were more abundant on $Ce_{0.75}Zr_{0.25}O_2$ than the

mononitrosyls, and exhibit distinctly lower reactivity toward co-adsorbed dioxygen in comparison to mononitrosyls. The O_2^- radicals formed initially on the Ce^{4+} ions are next stabilized on Zr^{4+}. Nitrates are the final product of surface reaction between nitrosyl complexes and dioxygen.

Acknowledgements

This work was carried out within the framework of the French-Polish collaboration Program Jumelage ''Materials for Environment'', and financially supported by The Polish State Committee for Scientific Research (Project no. 3 T09 147 26). The authors thank Jérémy Deremetz, Cécile Bonnevalle and Aurélie Martin (students from ENSCCF, France), who assisted at EPR experiments on NO_x and O_2 adsorption. Dr. Barbara Gil-Knap from the Faculty of Chemistry of the Jagiellonian University is kindly acknowledged for recording the IR spectra.

References

[1] J.N. Armor (Ed.), Environmental Catalysis, ACS, Washington, DC, 1994.
[2] A. Gervasini, P. Carniti, V. Ragaini, Appl. Catal. 22 (1999) 201.
[3] P. Forzatti, Appl. Catal. A 222 (2001) 221.
[4] M. Iwamoto, Stud. Surf. Sci. Catal. 130 (2000) 23.
[5] Y. Yokomichi, T. Yamabe, H. Otsuka, T. Kakumoto, J. Phys. Chem. 100 (1996) 14424.
[6] E. Giamello, D. Murphy, G. Magnacca, C. Morterra, Y. Shioya, T. Nomura, M. Anpo, J. Catal. 136 (1992) 510.
[7] K.A. Bethke, M.C. Kung, B. Yang, M. Shah, D. Alt, C. Li, H.H. Kung, Catal. Today 26 (1995) 169.
[8] E. Brocławik, J. Datka, B. Gil, W. Piskorz, P. Kozyra, Top. Catal. 11/12 (2000) 335.
[9] Z. Sojka, Appl. Magn. Reson. 18 (2000) 71.
[10] D. Pietrogiacomi, S. Tuti, M.C. Campa, V. Indovina, Appl. Catal. B 28 (2000) 43.
[11] R. Burch, E. Halpin, J.A. Sullivan, Appl. Catal. B 17 (1998) 115.
[12] A. Martínez-Arias, J. Soria, J.C. Conesa, X.L. Seoane, A. Arcoya, R. Cataluña, J. Chem. Soc., Faraday Trans. 91 (1995) 1679.
[13] P. Fornasiero, R. Di Monte, G. Ranga Rao, J. Kašpar, S. Meriani, A. Trovarelli, M. Graziani, J. Catal. 151 (1995) 168.
[14] M. Iwamoto, Stud. Surf. Sci. Catal. 130 (2000) 23.
[15] F. Garin, Appl. Catal. A 222 (2001) 183.
[16] T. Spalek, P. Pietrzyk, Z. Sojka, J. Chem. Inf. Model. 45 (2005) 18.
[17] A. Adamski, E. Tabor, B. Gil, Z. Sojka, Catal. Today (2006), in press.
[18] T. Rudolf, A. Pöppl, W. Brunner, D. Michel, Magn. Reson. Chem. 37 (1999) S93.
[19] R.D. Feltham, J.H. Enemark, Top. Stereochem. 12 (1981) 155.
[20] A. Volodin, D. Biglino, Y. Itgaki, M. Shiotani, A. Lund, Chem. Phys. Lett. 327 (2000) 165.
[21] A. Gutsze, M. Plato, H.G. Karge, F. Witzel, J. Chem. Soc., Faraday Trans. 92 (1996) 2495.
[22] H. Yahiro, A. Lund, R. Aasa, N.P. Benetis, M. Shiotani, J. Phys. Chem. A 104 (2000) 7950.
[23] K. Hadjiivanov, B. Tsyntsarski, T. Nikolova, PCCP 1 (1999) 4521.
[24] K.I. Hadjiivanov, Catal. Rev. Sci. Eng. 42 (2000) 71.
[25] P.C. Ford, I.M. Lorkovic, Chem. Rev. 102 (2002) 993.
[26] J. Datka, P. Kozyra, E. Kukulska-Zając, Catal. Today 90 (2004) 109.
[27] M. Kantcheva, A.S. Vakkasoglu, J. Catal. 223 (2004) 352.
[28] W. Känzig, K.H. Cohen, Phys. Rev. Lett. 3 (1959) 509.
[29] K. Dyrek, A. Adamski, Z. Sojka, Spectrochim. Acta A 54 (1998) 2337.